5.4 Stochastic analysis of an impact problem

Francisco Zárate
International Center for Numerical Methods in Engineering. Technical University of Catalonia, Barcelona, Spain

Jorge E. Hurtado
National University of Colombia, Manizales, Colombia

Eugenio Oñate
International Center for Numerical Methods in Engineering. Technical University of Catalonia, Barcelona, Spain

5.4.1 Introduction

Industrial pieces produced in series are characterized by imperfect geometry, as is well known. In some situations, such imperfections can have a serious effect on the overall mechanical behaviour of the piece. One of such situations is the impact of metallic bodies (Oñate, 1993) which has an increasing industrial interest. To analyze this problem there are several FE codes in the market. One of them is the SIMPACT code (CIMNE, 1997), which is used in the present example as a deterministic solver in a stochastic context. The problem at hand is to analyze the effect of geometrical imperfections, modelled as a random field (Hurtado and Barbat, 1998), on the behaviour of two cylinders of the same material under mutual impact. The purpose is to select the material that guarantees the best performance from a stochastic point of view.

Before entering into details, it should be pointed out that for this type of evaluation numerical methods exhibit a particular advantage over experimental ones. This is due to the fact that probabilistic assessments of any kind require large amounts of information, which can be very costly to obtain by an experimental way. Instead, the computation of several deterministic cases using random model parameters (i.e. the well known Monte Carlo method) allows the synthetic generation of the relevant response features without difficulty. This method of meta-computing (Marczyk, 1997) is extensively applied in the present case study, as explained in the following.

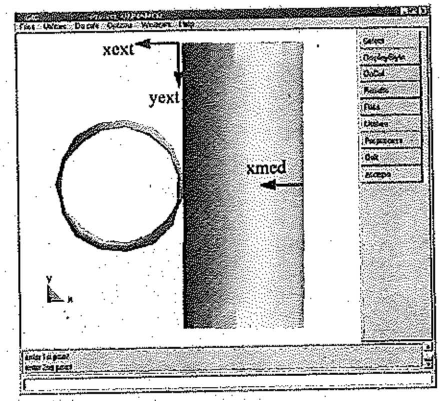

Figure 5.23: Impacting cylinders

5.4.2 Problem description

The case study deals with the stochastic analysis of the collision of two cylindrical tubes occurring at a right angle. One of them is idealized as a perfect cylinder with no geometrical imperfections and the other as the opposite case. Figure 5.23 depicts the geometry of the cylinders, where the geometrical imperfections are amplified for clarity reasons. The purpose of the study is to examine the effect of such imperfections on the overall behaviour of the tubes when varying the constituent material. The output variables of interest are the x and y components of the top displacement and the x component of the displacement at the middle of the tubes, i.e. the radial displacements of the external nodes diametrically opposite to the contact point in both cylinders.

Finite element model

Geometry

The main variables defining the geometry are the (nominal) radius $R_0 = 0.1$ m, the height $H = 0.46$ m and the thickness $t = 3$ mm for both cylinders. The random field used to model the initial radial imperfection in the geometry of one of the cylinders is given by Stam (Stam, 1996)

$$\bar{W} = t\bar{\xi}_1 \cos\frac{i\pi x}{H} + t\bar{\xi}_2 \sin\frac{k\pi x}{H}\cos\frac{ly}{R} \tag{5.18}$$

where $\bar{W}$ is the geometrical imperfection field, i is an integer describing the number of axial half waves, k is an integer describing the number of axial half waves in the asymmetric mode and l an integer characterizing the number of circumferential full waves. In the present example $i = 3$, $k = 2$ and $l = 4$. The parameters $\bar{\xi}_1, \bar{\xi}_2$ are the amplitudes of the axisymmetric and the asymmetric mode respectively. Thus the actual radius is

$$R_a = R_0 + \bar{W} \tag{5.19}$$

where R_0 is the nominal radius. Figure 5.24 shows the final stage of deformation of the two cylinders at 8 milliseconds after impact for one of the cases analyzed.

Mesh
Each cylinder was modelled with 150 three-node triangle elements BST (Cendoya, 1996; Zárate, 1996; Jovicevic, 1998) (a total of 300 triangles and 330 nodes). These elements account for plastic deformation by four integration layers through the thickness.

Materials
The materials considered in the simulation are steel and aluminium. The nominal properties of the steel are: Young's modulus $E = 210$ GPa, Poisson's ratio $\nu = 0.3$, initial yield stress $C = 200$ MPa. For the aluminium material, the nominal properties are: Young's modulus $E = 69$ GPa, Poisson's ratio $\nu = 0.33$ and the initial yield stress $C = 507$ MPa. Both materials are equiped with hardening properties. The mass density has been set equal to $\rho = 7840$ kg/m^3 with the aim of preserving the same kinetic energy. No boundary conditions are used in the study.

Loading
A velocity of 30 m/s was initially ascribed to all the nodes of both cylinders simultaneously, but oriented towards the other cylinder.

5.4.3 Analysis considerations

The total response time was arrived at by an automatic time stepping procedure. Material nonlinearities were considered to be rate independent and

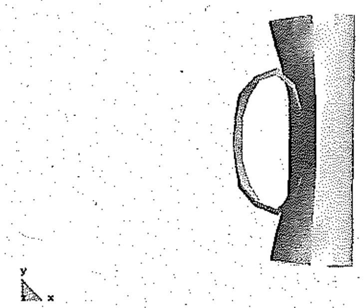

Figure 5.24: Final stage of deformation of the perfect versus imperfect cylinders.

the Updated Lagrangian Formulation was used to describe geometrical nonlinearities. A non-symmetric contact treatment is used, which means that the penetration is only checked at the nodes of the slave surface lying against the master ones. The frictional parameters of the contact surface are a static and a kinetic friction coefficient equal to 0.14 and 0.10, respectively.

5.4.4 Stochastic modelling

A critical step in designing a stochastic numerical experiment is the selection of the random variables (both input and output) out of the manifold that characterize a specific problem. Moreover, special care must be devoted to characterizing adequately the probability density function of the input random variables, as they govern completely the results. In case this information is absent, it is customary to use the normal (or Gaussian) density function in the spirit of the well known Central Limit Theorem.

In the present case, the random variable selected as dominant is the elasticity modulus, which was given a coefficient of variation of 0.1 for both materials. Besides, in modelling the imperfect contact surfaces, the imperfection amplitudes $\bar{\xi}_1$ and $\bar{\xi}_2$ were also considered as input random variables, where $\bar{\xi}_1$ is the axisymmetric amplitude and $\bar{\xi}_2$ is the asymmetric amplitude.

The normal density function was employed for both variables, with mean $\mu = 0.1$ and standard deviation $\sigma = 0.1$. The output variables are the radial displacement of the external nodes diametrically opposite to the contact point in both cylinders (*xmed* in Figure 5.23) and the radial and axial displacements of a point at the cylinder top (*xextr* and *yextr*, respectively).

The PROMENVIR meta-computing environment (PROMENVIR, 1997) has been used as the Monte Carlo analyzer, using the Finite Element code SIMPACT as a "workhorse" for performing the deterministic calculations. The Monte Carlo analysis comprised 430 sampling units for the steel tubes and 200 sampling units for the aluminium ones. The analysis was performed at CIMNE in Barcelona, using an SGI-Origin 2000 computer with four processors. The above synthetic sampling was carried out in two hours and 12 minutes in the case of the steel tubes and in one hour and three minutes in the case of the aluminium tubes.

5.4.5 Results and discussion

Once a PROMENVIR analysis has been run, the required information can be rapidly visualized by simply examining the ant-hill plots which are produced on-line as the calculation progresses. The amount of obtained engineering information is very impressive and it is described as follows.

Mean

The mean of the radial displacements of the nodes opposite to the contact point in both cylinders has been computed in order to be sure of the convergence of the sampling procedure. Notice that the mean corresponds to the most likely response in terms of radial displacements, so that it is of great engineering relevance. PROMENVIR provides two additional curves defining the width of the confidence interval of the mean. A typical example of such curves is shown in Figure 5.25, where it can be noticed that convergence has been achieved with nearly 250 shots.

Probabilistic interpretation

The criterion selected for a comparison of different cases is the Mahalanobis distance (see Chapter 2; Rencher, 1995). Is is defined within a single sample as

$$D_{\mathrm{M}}^2 = [\mathbf{y}_1 - \mathbf{y}_2]^{\mathrm{t}}\mathbf{S}^{-1}[\mathbf{y}_1 - \mathbf{y}_2] \qquad (5.20)$$

and measures the distance between two observations $\mathbf{y}_1$ and $\mathbf{y}_2$ in the random vector $\mathbf{y}$ of the output variables. The sample covariance matrix $\mathbf{S}$ is

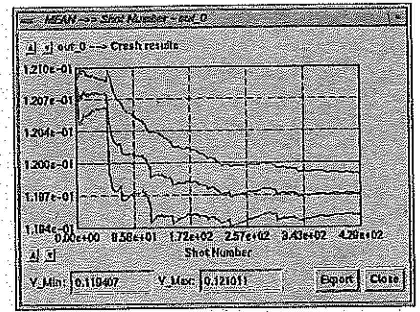

Figure 5.25: Mean of the radial displacement of the steel cylinder with imperfect geometry.

presumed non-singular. The distance $[\mathbf{y}_i - \overline{\mathbf{y}}]$ of observations $\mathbf{y}_i$ from the sample mean vector $\overline{\mathbf{y}}$ is equally determined.

Definition (5.20) can be extended to a measure of the distance between the mean vectors $\overline{\mathbf{y}}_1$ and $\overline{\mathbf{y}}_2$ of two samples,

$$D_{\mathrm{M}}^2 = [\overline{\mathbf{y}}_1 - \overline{\mathbf{y}}_2]^{\mathrm{t}}\mathbf{S}_{\mathrm{pl}}^{-1}[\overline{\mathbf{y}}_1 - \overline{\mathbf{y}}_2] \qquad (5.21)$$

in which case $\mathbf{S}_{\mathrm{pl}}$ is the pooled covariance matrix weighting the covariance matrices $\mathbf{S}_1$ and $\mathbf{S}_2$ of the two samples.

For a probabilistic analysis of the system of the impacting cylinders at hand, several case studies are feasible. If we are interested in the distance between the steel and the aluminium models of the perfect-imperfect impact under consideration, the indices "1" and "2" in eqn (5.21) are to be referred to the Monte Carlo samples for the steel and the aluminium materials, respectively. The random vector $\mathbf{y}$ comprises then the representative displacements of both the perfect and the imperfect cylinder.

An estimation of the effect of the imperfect geometry, on the other hand, would require consideration of four samples: impact of two perfect cylinders, and impact of two imperfect cylinders for each material the steel and the aluminium. Comparison of the "material" distances for the perfect system and for the imperfect system reveals the significance of the actually imperfect geometry for an assessment of the material selection.

The Monte Carlo data that have been obtained here for the perfect-imperfect system can be utilized for the determination of "conditional" distances. For instance, taking one of the materials (steel or aluminium) we distinguish two samples: one appertaining to the deformation of the perfect cylinder, the other appertaining to the imperfect cylinder. For this consideration, the random vectors $\mathbf{y}_1, \mathbf{y}_2$ refer to the representative displacements of each single cylinder, and so do the covariance matrices $\mathbf{S}_1, \mathbf{S}_2$ of the samples. Accordingly, eqn (5.21) determines the Mahalanobis distance between the mean vectors of the perfect and the imperfect geometry for the same material under the condition of this particular impact pairing.

In the following, we investigate with such a "conditional" distance the effect of geometry imperfections in assessing the material selection. To this end, the Mahalanobis distances between materials are listed in Table 5.3 as obtained for the perfect and for the imperfect cylinders in the impacting system. It is seen that consideration of the imperfections appearing in the actual configuration drastically reduces the statistical distance between the two materials. Although random field modelling makes the individuality of the materials less relevant, the distance remains large due to the difference in the properties. Another overall conclusion drawn from the observation of Figures 5.26 - 5.29 is that the scatter in the aluminium results (marked by crosses) is much higher than in the results for the steel material (marked by dots). This indicates a greater difficulty in applying quality control to the aluminium product, inasmuch as the larger the scatter the higher the probability of exceeding a performance threshold.

Table 5.3: Mahalanobis distances

Case 1	Case 2	D_{M}
Perfect steel	Perfect aluminium	31.02
Imperfect steel	Imperfect aluminium	10.72

Figures 5.26 and 5.27 depict Monte Carlo results for the perfect part of the system in steel and in aluminium. For the cylinder with perfect geometry the scatter is from the contact with its imperfect counterpart, on the one hand, and from the randomness of the elastic modulus, on the other hand. Despite the higher elastic modulus, the displacements on the top of the cylinder (the ends) in Figure 5.26 are larger for the steel material. This points to a prevelance of plastic deformations, since the yield stress for the steel has been taken by the factor 2.5 lower than for the aluminium. Accordingly, the randomness of the elastic modulus should be less important for the steel version.

From Figure 5.26, the axial and the radial displacements of the selected point at the ends are highly correlated for the steel. This indicates that deformation of the steel cylinder is by formation of a plastic yield mechanism. The behaviour of the same displacement components of the aluminium cylinder do not support such a relationship. In Figure 5.27, there is no correlation between the axial displacement on the top and the outer radial displacement in the middle cross-section for both the steel and the aluminium. The aluminium version exhibits a pronounced scatter in the radial direction. Again the moderate radial scatter for the steel at this position conforms with the prevelance of plastic deformations.

Figures 5.28 and 5.29 appertain to the imperfect cylinder in the system. The results maintain the functional relationships between displacements as in the perfect cylinder but the scatter is enhanced and leads to an apparent diminution of the (statistical) distance between the steel and the aluminium products.

5.4.6 Conclusions

Practically any structural problem when viewed from a stochastic perspective yields information that a deterministic approach will very rarely deliver. When scatter enters into the scene, one quickly realizes that much more may be understood about the system and its behaviour than after a single deterministic analysis. The main conclusions of the present study may be summarized as follows:

1. In the presence of geometry random fields, the difference in materials becomes less relevant than when modelling them with perfect geometry.

2. The scatter in the results for the aluminium case is higher than those of the steel one, thus making it less quality-controllable.

Acknowledgment

The authors wish to express their acknowledgments to Ioannis Doltsinis for his valuable comments on the probabilistic and mechanical interpretation of this case study.

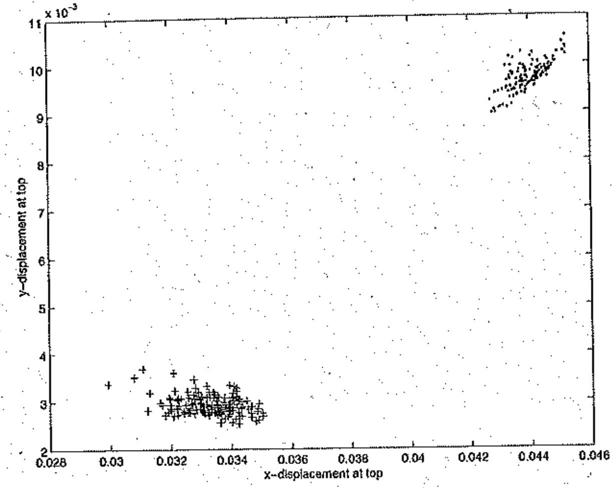

Figure 5.26: Clusters of perfect steel and aluminium cylinders.

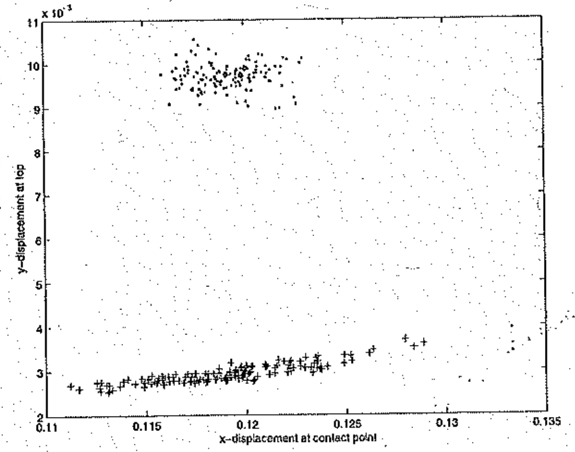

Figure 5.27: Clusters of perfect steel and aluminium cylinders.

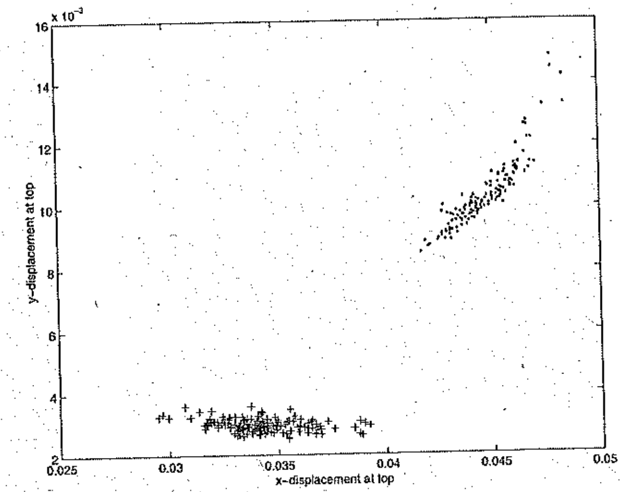

Figure 5.28: Clusters of imperfect steel and aluminium cylinders.

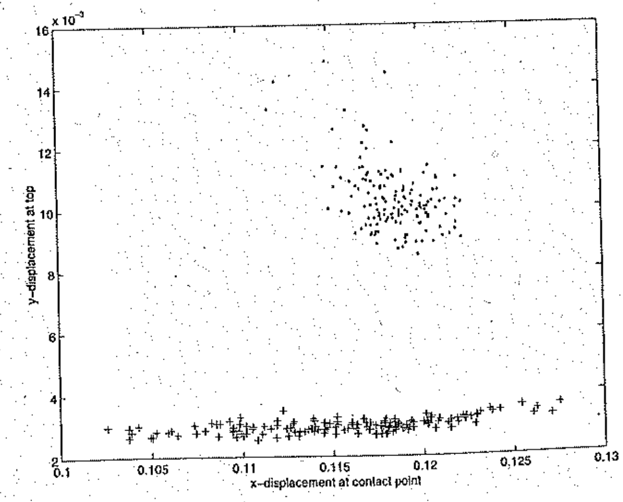

Figure 5.29: Clusters of imperfect steel and aluminium cylinders.